Canine Dilated Cardiomyopathy: Diffuse Remodeling, Focal Lesions, and the Involvement of Macrophages and New Vessel Formation

Gasparini, Stefania ; Fonfara, Sonja ; Kitz, Sarah ; Hetzel, Udo ; Kipar, Anja

Abstract: Dilated cardiomyopathy (DCM) is among the most common cardiac diseases in dogs. Its pathogenesis is not fully understood, but myocardial remodeling and inflammation are suspected to be involved. The present study aimed to characterize the pathological processes in canine DCM, investigating morphological changes in association with the expression of relevant cytokines and remodeling markers. The myocardium of 17 dogs with DCM and 6 dogs without cardiac diseases was histologically evaluated, and selected cases were further examined by immunohistochemistry, morphometry, and reverse transcription quantitative PCR. In DCM, the myocardium exhibited subtle but statistically significant diffuse quantitative changes. These comprised increased interstitial collagen deposition and macrophage numbers, as well as an overall reduced proportion of contractile tissue. This was accompanied by a significant increase in myocardial transcription of intracellular adhesion molecule (ICAM) 1, inflammatory cytokines, and remodeling enzymes. Laser microdissection showed that cardiomyocytes transcribed most relevant markers including ICAM-1, tumor necrosis factor , transforming growth factor (TGF-), matrix metalloproteinase 2 (MMP-2), tissue inhibitor of MMP (TIMP) 1 and TIMP-2. In addition, there were multifocal cell-rich lesions characterized by fibrosis, neovascularization, macrophage infiltration, and cardiomyocyte degeneration. In these, macrophages were often found to express ICAM-1, TGF- , and vascular endothelial growth factor; the former two were also expressed by cardiomyocytes. These results characterize the diffuse myocardial remodeling processes that occur in DCM. The observed multifocal cell-rich lesions might result from reduced tissue perfusion. Macrophages and cardiomyocytes seem to actively contribute to the remodeling processes, which ultimately lead to cardiac dilation and dysfunction. The precise role of the involved cells and the factors initiating the remodeling process still needs to be identified.

DOI: https://doi.org/10.1177/0300985820906895

Originally published at:
Gasparini, Stefania; Fonfara, Sonja; Kitz, Sarah; Hetzel, Udo; Kipar, Anja (2020). Canine Dilated Cardiomyopathy: Diffuse Remodeling, Focal Lesions, and the Involvement of Macrophages and New Vessel Formation. Veterinary Pathology, 57(3):397-408.
DOI: https://doi.org/10.1177/0300985820906895

Domestic Animals–Original Article

Veterinary Pathology
2020, Vol. 57(3) 397-408

DOI: 10.1177/0300985820906895
journals.sagepub.com/home/vet

Canine Dilated Cardiomyopathy: Diffuse Remodeling, Focal Lesions, and the Involvement of Macrophages and New Vessel Formation

Stefania Gasparini[1], Sonja Fonfara[2], Sarah Kitz[1], Udo Hetzel[1], and Anja Kipar[1]

Abstract

Dilated cardiomyopathy (DCM) is among the most common cardiac diseases in dogs. Its pathogenesis is not fully understood, but myocardial remodeling and inflammation are suspected to be involved. The present study aimed to characterize the pathological processes in canine DCM, investigating morphological changes in association with the expression of relevant cytokines and remodeling markers. The myocardium of 17 dogs with DCM and 6 dogs without cardiac diseases was histologically evaluated, and selected cases were further examined by immunohistochemistry, morphometry, and reverse transcription quantitative PCR. In DCM, the myocardium exhibited subtle but statistically significant diffuse quantitative changes. These comprised increased interstitial collagen deposition and macrophage numbers, as well as an overall reduced proportion of contractile tissue. This was accompanied by a significant increase in myocardial transcription of intracellular adhesion molecule (ICAM) 1, inflammatory cytokines, and remodeling enzymes. Laser microdissection showed that cardiomyocytes transcribed most relevant markers including ICAM-1, tumor necrosis factor α, transforming growth factor β (TGF-β), matrix metalloproteinase 2 (MMP-2), tissue inhibitor of MMP (TIMP) 1 and TIMP-2. In addition, there were multifocal cell-rich lesions characterized by fibrosis, neovascularization, macrophage infiltration, and cardiomyocyte degeneration. In these, macrophages were often found to express ICAM-1, TGF-β, and vascular endothelial growth factor; the former two were also expressed by cardiomyocytes. These results characterize the diffuse myocardial remodeling processes that occur in DCM. The observed multifocal cell-rich lesions might result from reduced tissue perfusion. Macrophages and cardiomyocytes seem to actively contribute to the remodeling processes, which ultimately lead to cardiac dilation and dysfunction. The precise role of the involved cells and the factors initiating the remodeling process still needs to be identified.

Keywords

canine dilated cardiomyopathy, dogs, fibrosis, heart, histology, immunohistochemistry, inflammation, macrophages, morphometry, myocardial remodeling

Dilated cardiomyopathy (DCM) is the most common cardiac disease in large-breed dogs and is characterized by cardiac chamber dilation, systolic dysfunction, and, in some cases, ventricular arrhythmia, which is eventually followed by congestive heart failure and/or sudden death.[38,48,52,56] The clinical diagnosis of DCM is based on echocardiographic findings and excluding other cardiac or systemic diseases and medications such as treatment with anthracycline[34] that may induce similar changes.[11,38,48,52]

Gross postmortem examination of the canine DCM heart reveals eccentric, primarily left ventricular hypertrophy and secondary left atrial dilation.[11,52] The histological changes, however, appear not to be very specific and are usually reported as mild: variation in myocyte size, myocyte degeneration and necrosis, and myocardial fibrosis of variable extent have been described.[4,13,28,43,55] According to the literature, 1 of 2 distinct histological patterns can predominate depending on the affected dog breed. The "fatty infiltration-degenerative" type, with myofiber degeneration, fibrosis, and adipocyte infiltration, is mainly described in Boxers and Doberman

[1]Institute of Veterinary Pathology, Vetsuisse Faculty, University of Zurich, Zurich, Switzerland
[2]Department of Clinical Studies, Ontario Veterinary College, University of Guelph, Guelph, Canada

Supplemental material for this article is available online.

Corresponding Author:
Anja Kipar, Institute of Veterinary Pathology, Vetsuisse Faculty, University of Zurich, Winterthurerstrasse 268, 8057 Zurich, Switzerland.
Email: anja.kipar@uzh.ch

Pinschers.[53] The "attenuated wavy fiber" type, with myofiber atrophy and a long wavy appearance of fibers, is typical of DCM in giant breeds but may also occur in Boxers and Doberman Pinschers.[53] More recent studies described further myocardial alterations, such as a change in the cardiomyocyte phenotype (reduced desmin expression), an increase in vimentin-positive cells in the left atrium, a mild mononuclear inflammatory infiltration in the interstitium of both atria and ventricular free walls,[27,28] and hypertrophy of coronary vessel walls.[29]

Progress has also been made regarding the etiology of DCM, and genes associated with the disease have been identified in Boxers, Doberman Pinschers, and Irish Wolfhounds.[39,40,42,48]

Following numerous studies conducted on small and large experimental animal models of both cardiomyopathies and myocardial infarction,[7,8,24] it is generally accepted that most pathological processes affecting the myocardium, including DCM, result in a sequence of structural and functional changes known as myocardial remodeling.[8,47] Myocardial remodeling is in general prompted by cardiomyocyte injury, followed by an inflammatory reaction that is mediated by different cell types, including neutrophils, macrophages, and lymphocytes, and regulated by several factors: proinflammatory cytokines, adhesion molecules, and extracellular matrix–degrading enzymes (eg, matrix metalloproteinases [MMPs]).[1,18,47] Anti-inflammatory cytokines and growth factors such as transforming growth factor β (TGF-β) are subsequently involved in the reparative phase, promoting differentiation of fibroblasts into myofibroblasts and extracellular matrix deposition.[5,9,18,19] However, this repair process can also result in excessive fibrosis.[18] Although sharing common pathways, depending on the type and extent of the initiating injury, different cellular and extracellular components are involved, and the outcome may vary.[3,47]

Recent studies by our group confirmed increased myocardial transcription of inflammatory cytokines, MMPs, and their inhibitors in dogs with cardiac diseases, suggesting a general activation of inflammatory responses in the myocardium in association with cardiac diseases.[15,16]

We hypothesized that the inflammatory and remodeling processes that are postulated to occur in the myocardium in association with canine DCM have consistent histopathological correlates in addition to those changes described so far. Therefore, the aim of the present study was to thoroughly assess the myocardium of dogs with clinically and grossly confirmed DCM for any pathological features and potential quantitative changes, to gain further information on the pathomechanisms underlying DCM.

Materials and Methods

Animals and Sample Collection

The study was conducted on the hearts of 23 dogs: 17 dogs with DCM and 6 dogs with diseases not involving the heart (control group) (Suppl. Tables S1 and S2). The dogs were all euthanized, except for dog No. 1.16, which suffered sudden death on a walk. Among the 17 dogs with DCM were 10 Great Danes, 6 Doberman Pinschers, and 1 Bullmastiff; they had a mean age of 6.4 years (range, 4–10 years). Nine dogs were female (4 of these were neutered) and 8 were male (of which 1 was neutered). The dogs in the control group represented various breeds and had a mean age of 7 years (range, 0.5–11 years), with 3 males and 3 females neutered.

At different time points prior to death, echocardiography had been carried out in all dogs with DCM to diagnose the disease, except for dog No. 1.16. For this dog, DCM was diagnosed on gross and histological cardiac findings during full necropsy. Further clinical investigations of the dogs with DCM had been performed at the discretion of the attending clinician (a board-certified cardiologist or a cardiology resident under direct supervision of a board-certified cardiologist) and included a complete blood count, biochemistry, electrocardiography, and/or thoracic radiographs, depending on patient presentation. Dogs with noncardiac diseases were euthanized on request of the owners due to grave prognoses (Suppl. Table S2). These dogs underwent investigations according to their presentation and based on the assessment of the attending clinician.

Dogs underwent a partial (thoracic cavity) diagnostic postmortem examination with the owners' consent. Hearts were removed and grossly examined for any pathological changes. Samples were collected from left atrium (LA) and right atrium (RA), left ventricular free wall (LV), right ventricular free wall (RV), and interventricular septum (IVS) for histological examination and, in selected cases (4 DCM and all control dogs), for RNA extraction (Suppl. Tables S1 and S2). For the latter, to obtain samples of the atria, these were opened and 3 to 4 samples of around 3 to 5 mm in length were collected from the central part of the LA and RA and placed in RNAlater (Thermo Fisher, Waltham, MA). For the ventricular samples, the lower half of the heart was separated by a cross section, and 2 to 3 samples of around 5 mm length in each direction (if the LV was thicker than 5 mm, a thinner slice was taken to ensure saturation with RNAlater) was obtained from each of the middle LV, IVS, and RV myocardium toward the heart base and placed in RNAlater. For histology, LA and RA were laminated vertically to produce ring-shaped cross sections that allowed dorsoventral orientation of the specimens in the cassette. One cross-sectional slice of the removed apex was processed, and longitudinal sections were prepared from the lateral quadrant of the LV and RV, including the atrioventricular valves and ventricular papillary muscles. Samples of the IVS were taken from the center, between heart base and apex, stretching from the anterior epicardium to the middle of the IVS muscle.

Histological, Immunohistochemical, and Fluorescence Examinations

Myocardial samples were fixed in 10% neutral-buffered formalin and routinely embedded in paraffin wax. Consecutive sections (3–5 µm) were prepared and routinely stained with hematoxylin and eosin and the van Gieson (VG) stain for the demonstration of collagen. In 15 DCM cases (Suppl. Table S1) and all control hearts, additional sections were subjected to immunohistochemistry and fluorescence staining.

The specimens were evaluated by light microscopy and assessed for any histopathological changes, including those previously described in DCM, such as fatty infiltration, wavy fibers, fibrosis, and cardiomyocyte necrosis/degeneration.[53]

Immunohistochemistry was performed using a Dako autostainer (Dako, Glostrup, Denmark) or the Discovery XT autostainer (Ventana Medical System, Tucson, AZ) to detect leukocytes ($CD18^+$, Major Histocompatibility Complex (MHC) II^+), specifically, T cells ($CD3^+$), B cells ($CD20^+$), macrophages (calprotectin$^+$, $CD18^+$, Iba-1^+), blood vessels (ie, vascular endothelial cells [factor $VIII^+$, $CD31^+$]) and smooth muscle cells (α–smooth muscle actin [α-SMA]$^+$), and relevant mediators (ie, TGF-β1, vascular endothelial growth factor [VEGF] and its receptor [Flk-1] and intercellular adhesion molecule 1 [ICAM-1]). Immunohistochemistry methods are listed in Supplemental Table S3. Briefly, after deparaffination, antigen retrieval was performed for all antigens except for α-SMA and CD20, by incubation of the slides with citrate buffer (pH 6) at 98°C for 10 minutes or with EDTA buffer (pH 9) at 98°C for 20 minutes. Endogenous peroxidase was blocked by incubation with hydrogen peroxide solution for 10 minutes. Sections were incubated with horse serum for 30 minutes at room temperature, followed by the primary antibodies and matching secondary antibodies; different detection kits were then applied. Sections were washed with phosphate-buffered saline between each incubation step (pH 8). Finally, sections were counterstained with hematoxylin for 40 seconds and mounted.

Consecutive sections incubated with an isotype-matched irrelevant antibody or without the primary antibody served as negative controls. A chronic inflammatory process with granulation tissue formation served as positive control tissue.

The immunohistochemical staining was evaluated based on the morphology and location of the positive cells (vascular endothelial cells, smooth muscle cells in vessel wall, interstitial cells, lymphocytes, and cardiomyocytes) as well as their distribution (scattered, multifocal, or diffuse).

A further section underwent fluorescence staining to mark cell nuclei, using the ProLong Diamond Antifade Mountant with DAPI (4′,6-diamidino-2-phenylindole; Invitrogen, Carlsbad, CA). Briefly, after deparaffination and rehydration, sections were incubated with DAPI for 24 hours at room temperature in the dark and then mounted.

Histomorphometric Analysis

Sections from RV, LV, and IVS from 15 dogs with DCM (Suppl. Table S1) and from all control dogs (Suppl. Table S2) that were stained with the VG stain, DAPI fluorescence, and immunohistochemistry for α-SMA and Iba-1 and exhibited consistent staining quality throughout the entire section were scanned (NanoZoomer-XR C12000; Hamamatsu, Hamamatsu City, Japan) to obtain high-resolution digital images. These were subsequently analyzed with the Visiopharm Integrator System (VIS, version 4.5.1.324; Visiopharm, Hørsholm, Denmark), considering the following parameters: overall cell number (based on the number of DAPI-positive nuclei), percentage area occupied by collagen fibers (based on the percentage of VG-positive fibers), number of interstitial macrophages and blood vessels (based on the number of Iba-1- and α-SMA-positive cells, respectively), and the respective proportion of tissue occupied by (a) cardiomyocytes (interpreted as contractile tissue), (b) collagen fibers, and (c) fiber- and cell-free interstitial space (all assessed in the VG-stained section). To specify, for each section, regions of interest with a size of 0.237 mm^2 (the area of a high-power field with 1 ocular of 22 mm field of view) were randomly selected across the myocardium from areas free of focal cell-rich lesions. For DAPI, α-SMA and Iba-1, and VG, positive cells and percentage of VG-positive fibers were counted in 20 regions of interest per section. In the VG-stained sections, the areas composed of (a) cardiomyocytes, (b) collagen fibers, and (c) fiber- and cell-free interstitial space were quantified within 10 regions of interest per section.

Relative Quantification of Cytokine and Remodeling Marker Transcription

From selected DCM cases (Nos. 1.10, 1.11, 1.14, and 1.15; Suppl. Table S1) and the control dogs (which were partly used in previous studies[15,16]), myocardial samples were collected within 1 hour after death. These were stored in RNAlater at –20°C until further use. Reverse transcriptase quantitative polymerase chain reaction (RT-qPCR) was carried out as previously described.[17] Published primer sequences were used for the canine housekeeping gene GAPDH; ICAM-1; cytokines (interleukin [IL]–1, IL-6, IL-8, IL-10; tumor necrosis factor α [TNF-α]; TGF-β); MMP–1, MMP-2, MMP-3, MMP-9, and MMP-13; tissue inhibitor of MMP (TIMP)–1, TIMP-2, TIMP-3, and TIMP-4; and lysyl oxidase.[15,16,41] As previously reported, the primer efficiencies were between 95% and 118%.[15,16] The relative transcription levels of all markers were calculated using GAPDH and the $2^{-\Delta Ct}$ method, as previously reported; all dogs have been part of previous studies, the results of which have been published in different contexts.[15,16] From 1 dog with DCM (dog No. 1.10), cardiomyocytes were collected using laser microdissection; RNA was extracted and qPCR was carried out as previously reported.[15,16]

Statistical Analyses

Statistical analysis was carried out using SPSS (SPSS, Inc, an IBM Company, Chicago, IL). Distribution of data obtained from histomorphometry and qPCR was analyzed applying graphical Q-Q plots and Kolmogorov-Smirnov and Shapiro-Wilk tests. Data were not normally distributed for α-SMA, VG, ICAM-1, cytokines, MMP, and TIMPs. Results from dogs with DCM and control dogs and results for different cardiac regions were therefore compared using Kruskal-Wallis and Mann-

Whitney U tests for nonnormally distributed data and 1-way analysis of variance (ANOVA) and unpaired t tests for normally distributed data. Statistical significance was defined as $P < .05$.

Results

Study Population

Dogs with DCM were Great Danes ($n = 10$), Doberman Pinschers ($n = 6$), and 1 Bull Mastiff; the 6 control dogs were all of different breeds. With a mean (SD) age of 6.4 (1.6) and 7 (3.6) years, respectively, dogs with DCM and control dogs were of similar age ($P = .531$). Among the dogs with DCM, the Great Danes had a mean (SD) age of 6 (1.5) years and were overall slightly younger than the Doberman Pinschers, which had a mean (SD) age of 7 (1.8) years. However, the age difference was not significant ($P = .247$).

Gross Findings

Grossly, the hearts from all dogs with DCM showed the previously reported macroscopic changes,[11,52] that is, cardiomegaly and chamber dilation (primarily of LA and LV). The hearts of control dogs were macroscopically unremarkable.

The DCM Myocardium Exhibits Diffuse Widening of the Interstitium With Increase in Collagen Deposition and Macrophages and Relative Reduction of the Contractile Tissue

All hearts were first screened for the presence of those histological features of DCM that are known from the literature.[11,37,53] Changes consistent with the fatty infiltration-degenerative type were disseminated in the LV and/or IVS in 12 DCM cases (6/6 Doberman Pinschers, 5/10 Great Danes, 1/1 Bullmastiff) and also in the RA, RV, or LA in half of the cases ($n = 6$; 4 Doberman Pinschers, 1 Great Dane, and the Bullmastiff). Changes consistent with the attenuated wavy fiber type, represented by multifocal areas with thin myofibers that showed a wavy appearance, were detected only in Great Danes (7/10), most frequently in the RA ($n = 5$), followed by the RV ($n = 3$) and LV and IVS (each $n = 2$). The results are listed in Supplemental Table S1. Neither change was observed in the control hearts.

In 5 of 17 DCM dogs (4 Great Danes and 1 Doberman Pinscher; dog Nos. 1.1, 1.2, 1.6, 1.10, 1.12), there were vascular changes represented by mild medial hypertrophy of intramural arteries.[13,29] A focal chronic mural thrombus was detected in the LA of 1 Great Dane (dog No. 1.10).

In comparison to the myocardium of the control dogs, the interstitium of the DCM myocardium appeared overall diffusely wider and more cellular (Figs. 1, 2). In most cases, this finding was most prominent in the LV and IVS. The interstitial cells were generally round to spindle shaped, with a moderate to high amount of cytoplasm and oval to round nuclei. Some were more slender and resembled fibroblasts but did not appear associated with collagen deposition (Fig. 3). Regardless of their shape, the majority of these cells were identified as macrophages, as they were found to express Iba-1, CD18, and MHC II (Fig. 4a–c). Occasional intact cardiomyocytes distant from lesions exhibited strong cytoplasmic MHC II expression (data not shown). Calprotectin expression was observed in monocytes within vessel lumina and in occasional elongated interstitial cells, suggesting these had recently emigrated from the blood into the tissue.[18] A small proportion of the spindle-shaped cells showed α-SMA expression (Fig. 5a). Otherwise, α-SMA-positive cells were seen to surround small blood vessels, as confirmed by the matching arrangement of endothelial cells (FVIII-related antigen$^+$; Fig. 5b); the latter were found to occasionally express Iba-1 and MHC II (Fig. 4a,c). Occasional individual T cells (CD3$^+$) and B cells (CD20$^+$) were also seen.

Apart from the above-mentioned occasional "wavy fibers" and mild degenerative changes (rare loss of striation and scattered cytoplasmic vacuolization), the cardiomyocytes appeared unaltered.

A morphometric approach was taken to substantiate the above findings. Assessment of the control dogs showed that in all examined cardiac regions (ie, LV, RV, IVS), the myocardium was similar with respect to the overall cellularity (DAPI$^+$ nuclei), proportion of contractile tissue, interstitial width (optically empty space plus collagen fibers), and the amount of small vessels (α-SMA$^+$ vascular structures) and macrophages (Iba-1$^+$) in the interstitium (Table 1).

In DCM, the myocardium exhibited an overall significantly lower cellularity (DAPI$^+$ nuclei) than in control dogs. This was coupled with a significant increase in the number of Iba-1$^+$ interstitial macrophages and a significantly lower relative proportion of contractile tissue, as well as an increased proportion of both fiber- and cell-free interstitial space and interstitial collagen (Table 2).

A comparison of these parameters in the different cardiac regions (LV, RV, IVS) of dogs with DCM and control dogs confirmed these results. The proportion of fiber- and cell-free interstitial space was significantly increased and the proportion of contractile tissue was significantly reduced in all 3 regions in DCM dogs (Table 1). Similarly, DCM dogs also exhibited a decreased overall cellularity and an increase in interstitial collagen, but the difference was significant only in the LV and IVS. Interestingly, the amount of Iba-1$^+$ interstitial macrophages was increased in both LV and IVS, but the difference was only significant in the LV (Table 1). A comparison of the different cardiac regions in DCM also showed region-dependent differences for several parameters. The number of interstitial macrophages (Iba-1$^+$) was significantly higher in the LV and IVS than in the RV. The interstitial collagen content was higher in the LV than in the IVS, whereas the proportion of contractile tissue (area covered by cardiomyocytes) was higher in the IVS than in the LV (Table 1).

There was no significant difference in the number of interstitial vessels (α-SMA$^+$ structures) between both groups of dogs and in the different cardiac regions in both groups (Tables 1, 2).

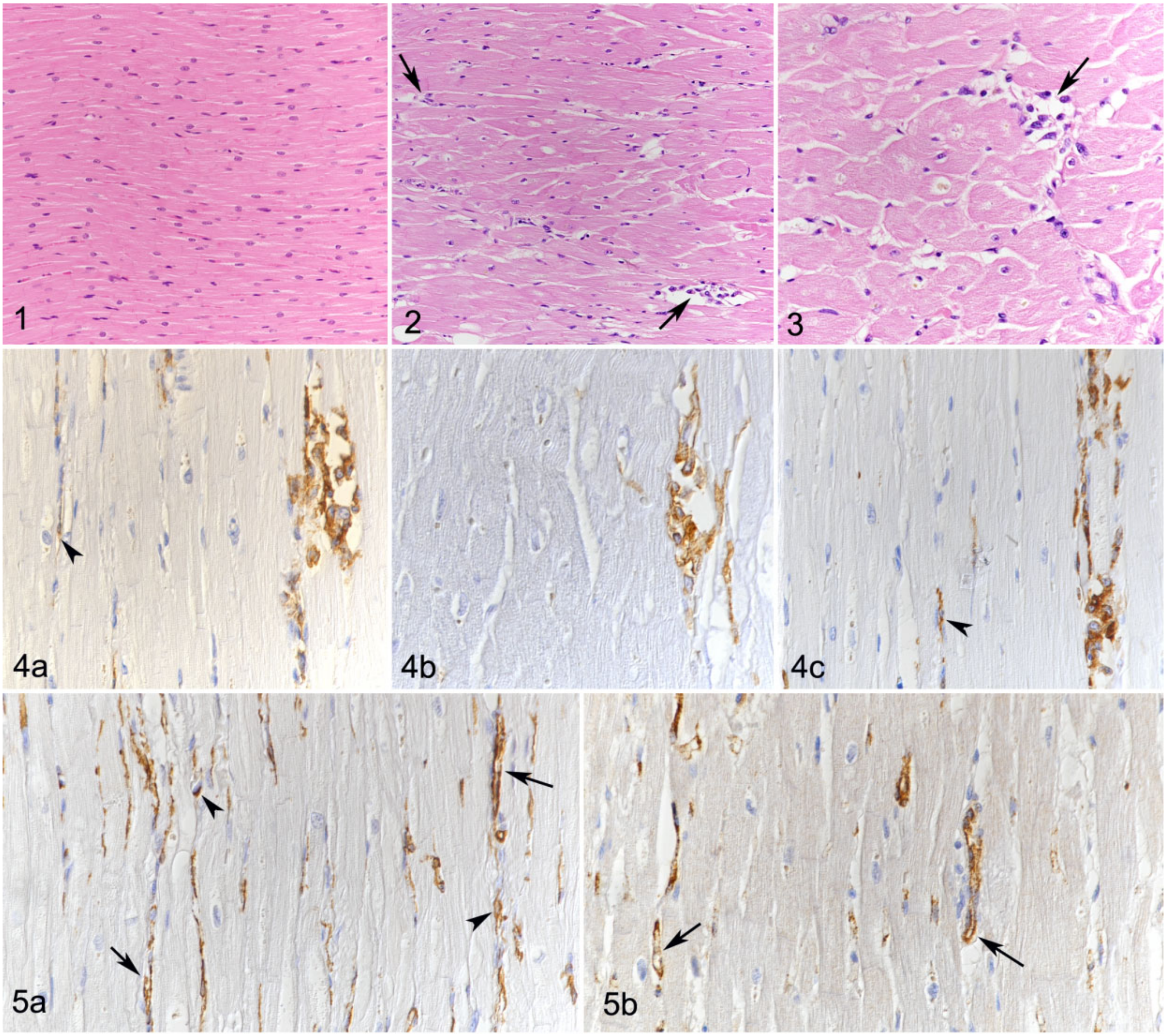

Figure 1. Control heart, dog No. 2.3. Unaltered myocardium with tightly aligned cardiomyocytes. Hematoxylin and eosin (HE). **Figures 2–5.** Dilated cardiomyopathy, heart, dog No. 1.15. **Figure 2.** The myocardium exhibits a widened interstitium with an increased amount of cells (arrow). HE. **Figure 3.** The interstitial cells (arrow) are round to spindle shaped, with an oval to round nucleus, sometimes more slender, resembling fibroblasts. HE. **Figure 4.** The majority of interstitial cells are macrophages, as they express ionized calcium binding adaptor molecule 1 (Iba-1) (a), CD18 (b), and Major Histocompatibility Complex (MHC) II (c). Occasional endothelial cells (arrowheads) in interstitial vessels express Iba-1 (a) and/or MHC II (c). Immunohistochemistry, hematoxylin counterstain. **Figure 5.** The interstitium exhibits abundant small vessels, identified by an outer layer of α–smooth muscle actin (α-SMA)–positive cells (smooth muscle cells, arrows) (a) and an inner FVIII-related antigen-positive endothelial cell layer (b). A small proportion of the spindle-shaped cells in the interstitium also show α-SMA expression (myofibroblasts; arrowheads) (a). Immunohistochemistry, hematoxylin counterstain.

The DCM Myocardium Exhibits Focal Lesions, Representing Areas of Fibroblast and Macrophage Accumulation and New Vessel Formation

In 14 DCM cases, focal to multifocal, occasionally coalescing lesions, ranging between approximately 0.1 and 5 mm in diameter (Fig. 6a), were found in addition to the diffuse changes described above. These consisted of focal expansion of the interstitium and replacement of cardiomyocytes by cell-rich infiltrates containing differentiated vessels and abundant round to elongate cells with a morphology similar to the interstitial cells described above (Fig. 6b). A large proportion of these cells were identified as macrophages (Iba-1^+, $CD18^+$, MHC II^+) (Fig. 7a–c). However, staining for α-SMA revealed that

Table 1. Comparison of Overall Cellularity, Number of Interstitial Small Vessels, and Macrophages, and Percentage of Area Covered by Cardiomyocytes, Collagen, and Fiber- and Cell-Free Interstitial Space in the Myocardium of the Different Cardiac Regions (Right and Left Ventricle and Interventricular Septum) of Control Dogs and Dogs With DCM.[a]

	Control			DCM			
Parameters	RV (n = 5)	IVS (n = 5)	LV (n = 6)	RV (n = 5)	IVS (n = 8)	LV (n = 11)	P Value
DAPI	1005 (319)	1014^{1} (237)	988^{2} (298)	744 (80.0)	760^{1} (147.8)	768^{2} (127.8)	$.035,^{1}$ $.048^{2}$
α-SMA	791 (310–1066)	926 (411–972)	901 (553–947)	706 (512–1167)	735 (459–1125)	724 (434–1214)	
Collagen	1.53 (1.06–2.03)	1.05^{1} (0.15–1.61)	0.95^{2} (0.18–1.87)	1.91 (1.02–8.46)	$2.29^{1,3}$ (1.12–6.62)	$4.51^{2,3}$ (1.54–12.37)	$.002,^{1}$ $.07,^{2}$ $.02^{3}$
Iba-1	59.8 (29.8)	53.8 (26.9)	46.6^{1} (11.7)	$37.2^{2,3}$ (23.9)	81.9^{2} (35.1)	$83.0^{1,3}$ (27.1)	$.02,^{1}$ $.03,^{2}$ $.006^{3}$
Cardiomyocytes	86.8^{1} (4.4)	90.5^{2} (3.3)	89.3^{3} (6.1)	66.3^{1} (12.4)	$73.6^{2,4}$ (10.4)	$63.2^{3,4}$ (7.2)	$.008,^{1}$ $.002,^{2}$ $<.01,^{3}$ $.02^{4}$
Interstitial space	11.7^{1} (4.0)	8.8^{2} (3.4)	9.7^{3} (5.7)	30.6^{1} (10.5)	24.9^{2} (10.2)	31.8^{3} (6.6)	$.006,^{1}$ $.003,^{2}$ $<.01^{3}$

Abbreviations: α-SMA, α–smooth muscle actin; DAPI, 4′,6-diamidino-2-phenylindole; DCM, dilated cardiomyopathy; Iba-1, ionized calcium binding adaptor molecule 1; IVS, interventricular septum; LV, left ventricle; RV, right ventricle.

[a]Results in each row that are significantly different from each other are marked by the same superscript number. Normal distributed results are reported as mean (standard deviation); not normal distributed data are reported as median (interquartile range). DAPI, number of cells per 20 regions of interest (ROI), based on the number of DAPI-positive fluorescent nuclei; α-SMA, number of vessels per 20 ROIs, based on the number of α-SMA positive vascular structures; Collagen, percentage area occupied by VG-positive fibers in 20 ROIs; Iba-1, number of macrophages per 20 ROIs, based on the number of Iba-1-positive interstitial cells; Cardiomyocytes, percentage area occupied by cardiomyocytes in 10 ROIs in VG-stained section; Interstitial space, percentage area of fiber- and cell-free interstitial space in 10 ROIs in VG-stained section.

Table 2. Comparison of Overall Cellularity, Number of Interstitial Small Vessels, and Macrophages, and Percentage of Area Covered by Cardiomyocytes, Collagen, and Fiber- and Cell-Free Interstitial Space in the Myocardium (Right and Left Ventricle and Interventricular Septum) of Control Dogs and Dogs With DCM.[a]

Parameters	Control (n = 14)	DCM (n = 23)	P Value
DAPI	1002 (268)	761 ↓ (124)	.003
α-SMA	920 (310–1066)	724 (434–1214)	.72
Collagen	1.17 (0.15–2.03)	3.08 ↑ (1.02–12.37)	<.001
Iba-1	53.4 (23.1)	73.1 ↑ (33.9)	.038
Cardiomyocytes	88.9 (4.8)	67.3 ↓ (10.2)	<.001
Interstitial space	10.0 (4.4)	29.2 ↑ (8.9)	<.001

Abbreviations: α-SMA, α–smooth muscle actin; DAPI, 4′,6-diamidino-2-phenylindole; DCM, dilated cardiomyopathy; Iba-1, ionized calcium binding adaptor molecule 1; IVS, interventricular septum; LV, left ventricle; RV, right ventricle.

[a]Overall assessment based on the available data for all 3 cardiac regions. Normal distributed results are reported as mean (standard deviation); not normal distributed data are reported as median (interquartile range).

the infiltrates also contained large amounts of small vessels (ranging in diameter between approximately 10 and 50 μm; Fig. 7d). This was confirmed by staining for FVIII-related antigen and CD31, both highlighting the inner ring of endothelial cells and the presence of a small vascular lumen. The endothelial cells were occasionally found to also express Iba-1 (Fig. 7a) and MHC II (Fig. 7c). Vessels clearly dominated in some areas of the lesions (Fig. 8). Collagen fibers were found in small amounts between the cells within the lesions and replacing or surrounding individual degenerated cardiomyocytes. The fibers were generally thin and loosely arranged, rarely forming more mature, dense fibrous tissue deposits (Fig. 9). Residual cardiomyocytes entrapped within the lesions displayed degenerative changes (swollen and vacuolated sarcoplasm) or necrosis. These lesions were most frequent in the LV (12/17), IVS (6/17), and RA (5/17) (Suppl. Table S1). In the control dogs, the myocardium did not exhibit any of the above described histological changes.

The Pathological Changes in the DCM Myocardium Are Associated With Significant Upregulation of Cytokines and Remodeling Markers

As previously described, the normal canine myocardium exhibits constitutive expression of cytokines and remodeling markers.[15,16] In the present study, we showed that this is also true for the adhesion molecule ICAM-1. In comparison, dogs with DCM showed significantly higher myocardial transcription of ICAM-1, TNF-α, IL-1, IL-8, IL-10, MMP-2, TIMP-1, and lysyl oxidase (Table 3). Laser microdissection with subsequent qPCR from 1 dog indicated that cardiomyocytes have gene expression of all markers tested with this approach (ie, ICAM-1, TNF-α, IL-8, TGF-β, MMP-2, TIMP-1, and TIMP-2). For ICAM-1 and TGF-β, immunohistochemistry was also applied and confirmed that morphologically unaltered cardiomyocytes produce both proteins, at low (ICAM-1) and very low

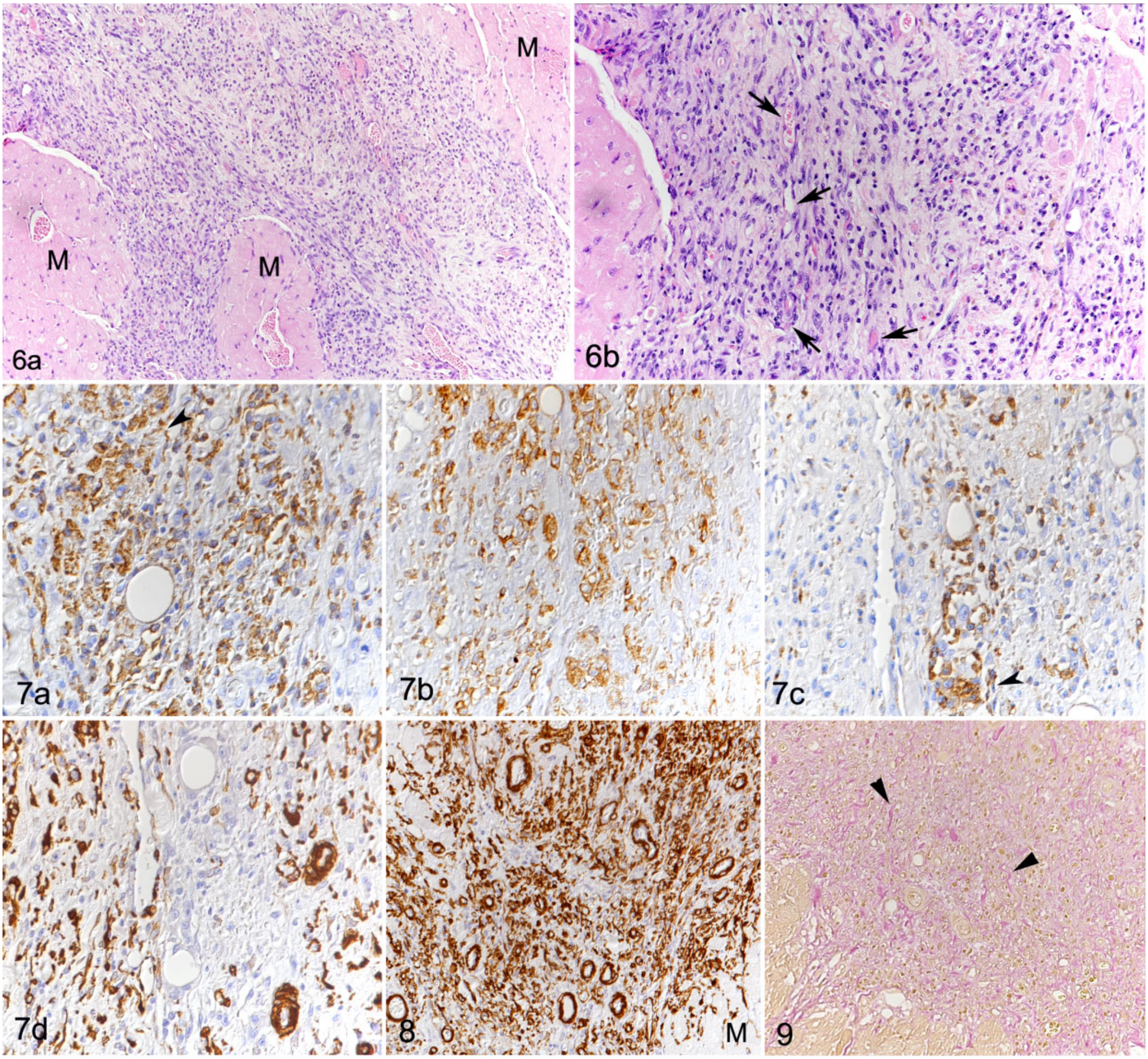

Figures 6–9. Dilated cardiomyopathy, heart, dog No. 1.15. Focal lesions. **Figure 6.** (a) Focal replacement of cardiomyocytes by a cell-rich infiltrate. M, myocardium with unaltered cardiomyocytes. (b) The infiltrate contains differentiated vessels (arrows) and abundant round to elongate cells with a morphology similar to the interstitial cells that were observed in increased numbers throughout the entire myocardium. Hematoxylin and eosin (HE). **Figure 7.** A large proportion of cells in the infiltrate are identified as macrophages, based on the expression of ionized calcium binding adaptor molecule 1 (Iba-1) (a), CD18 (b), and major histocompatibility complex (MHC) II (c), intermingled with and slightly outnumbering the α–smooth muscle actin (α-SMA)–positive cells that mainly form small vessels (d). Occasional endothelial cells also express Iba-1 (a; arrowhead) and MHC II (c; arrowhead). Immunohistochemistry, hematoxylin counterstain. **Figure 8.** Vessels clearly dominated in some areas of the lesions. Immunohistochemistry for α-SMA, hematoxylin counterstain. **Figure 9.** Small amounts of predominantly thin and loosely arranged collagen (arrowheads) between the cells within the lesions. Van Gieson.

(TGF-β) levels in control hearts, and moderately (ICAM-1) and weakly (TGF-β) in DCM (Figs. 10–15). VEGF and its receptor, Flk1, were not expressed in the myocardium of control dogs, and VEGF expression was not detected in cardiomyocytes in DCM either (Figs. 16, 17). However, Flk1 was consistently expressed by cardiomyocytes in DCM (Figs. 18, 19). ICAM-1, TGF-β, and VEGF were also expressed in a proportion of cells within the focal lesions, mainly with the morphology of macrophages (Figs. 12, 15, 17). Interestingly, the mononuclear cells in the interstitium were often strongly TGF-β positive (Fig. 14) but showed only weak ICAM-1 (Fig. 11) and neither VEGF nor Flk1 expression (Figs. 16, 18). Endothelial cells of

Table 3. Relative Messenger RNA Expression of ICAM-1, Cytokines, and Remodeling Markers in the Myocardium of Control Dogs and Dogs With DCM.[a]

Marker	Control ($n = 30^{b}$)	DCM ($n = 20^{b}$)	*P* Value
ICAM	298 (107–761)	1277 ↑ (255–3934)	**.003**
IL-1	7.6 (4.5–23.8)	19.4 ↑ (11.7–32.3)	**.012**
IL-6	10.02 (3.23–24.2)	71.3 (6.97–144)	.075
IL-8	47.2 (26.1–119.4)	232 ↑ (71.6–811)	**.001**
IL-10	19.5 (12.8–38.3)	48.7 ↑ (32.1–153)	**<.001**
TNF-α	4.14 (2.75–6.83)	12.4 ↑ (3.05–19.6)	**.019**
TGF-β	3457 (1977–4960)	3555 (2622–4780)	.406
MMP-1	1.97 (0.3–10.9)	2.49 (0.2–21.2)	.621
MMP-2	230 (52.4–386.2)	980 ↑ (318.6–2033.4)	**<.001**
MMP-3	0.11 (0.0–1.7)	0.12 (0.0–0.53)	.338
MMP-9	9.1 (1.5–28.6)	3.4 (1.6–61.6)	.890
MMP-13	0.64 (0.18–1.41)	1.37 (0.75–3.88)	.053
TIMP-1	401 (229–1212)	1173 ↑ (513–7563)	**.002**
TIMP-2	6801 (4783–9615)	10510 (5516–18 408)	.055
TIMP-3	18 655 (6910–27 788)	11 735 (5071–20 188)	.075
TIMP-4	1777 (1325–3478)	3347 (1609–4878)	.175
Lysyl oxidase	889 (403–1805)	1795 ↑ (1078–3252)	**.009**

Abbreviations: DCM, dilated cardiomyopathy; ICAM, intercellular adhesion molecule 1; IL, interleukin; MMP, matrix metalloproteinase; TGF, transforming growth factor; TIMP, tissue inhibitor of metalloproteinases; TNF, tumor necrosis factor.

[a] Relative expression using the Ct value of the respective marker to the Ct value of GAPDH was applied, $2^{-\Delta Ct}$. Results are reported as median (interquartile range).

[b] Total number of samples (left atrium, right atrium, left ventricle, interventricular septum, and right ventricle) examined for this group. *P* values indicating significant differences are in bold.

both intralesional and extralesional vessels occasionally showed weak ICAM-1, TGF-β, and Flk1 expression. A similar expression was seen occasionally in vessels in the control hearts.

Discussion

The present study represents a detailed investigation into the pathological changes of canine DCM, a disease associated with cardiac remodeling and of largely unknown pathogenesis.[29,47,51] Our results confirm a number of previously described histological changes as consistent features of canine DCM.[53] The so-called fatty infiltration-degenerative type was primarily found in Doberman Pinschers and the Bullmastiff.[53] These dogs did not show changes consistent with the attenuated wavy fiber type. Great Danes, on the other hand, exhibited either fatty infiltration-degenerative or attenuated wavy fiber type changes, or both. Similar to previously published studies, these results suggest breed-dependent differences in the underlying pathogenesis or in the cardiomyocyte response to injury,[54] which might also be the cause of breed differences in clinical presentations.[48,55] Interestingly, fatty infiltration-degenerative type changes were found to affect both the left and right heart, whereas attenuated wavy fiber type changes were more prominent in the right (RA and RV); this differs from a previous study undertaken in several dog breeds that reported wavy fibers as most abundant in the LV.[53]

Besides these known morphological features, the present study revealed more subtle diffuse myocardial changes in all DCM hearts and, in addition, cell-rich focal lesions in a large proportion of cases, both without any relation to the presence of attenuated wavy fiber or fatty infiltration-degenerative type changes. To specify, the diffuse changes consisted of a relative reduction of the contractile tissue in association with an expansion of the interstitium due to an overall widening of the fiber- and cell-free space and an increase in the amount of interstitial collagen. Alongside this, an overall significantly reduced cellularity was observed despite a significant increase in interstitial macrophages (Iba1^{+}); this indicates that DCM is associated with loss of cardiomyocytes and thereby of contractile tissue.

Taken together, these findings point toward individual cardiomyocyte injury and loss as the initial pathogenic process. This suggests that canine DCM differs from human primary DCM where the overall cell number does not change and an increase in cardiac muscle mass is observed as a result of compensatory cardiomyocyte hypertrophy.[2] Further detailed studies would be required to confirm that canine DCM is indeed not associated with a change in cardiomyocyte size.

The focal cell-rich lesions were found more or less randomly distributed in most (14/17) DCM hearts, where they were most prevalent and intense in the LV, followed by the IVS. Macrophages (Iba-1^{+}, CD18^{+}, MHC II^{+}) were also abundant in these lesions. Both here and in the interstitium, the macrophages could be the result of local proliferation of resident cardiac macrophages and of monocyte recruitment.[22,26] Since calprotectin, a myeloid cell marker expressed by neutrophils, monocytes, and recently blood-derived but not mature macrophages,[18] was found to be expressed only rarely in myocardial macrophages, it is likely that the vast majority were tissue-resident macrophages or resulted from local proliferation of macrophages recruited at an earlier stage.[32] Given the large heterogeneity of macrophage phenotypes and functions,[12,20,23] it is not clear if macrophages involved in the response to cardiac injury have a proinflammatory role and contribute to adverse cardiac remodeling or have instead a reparative and cardioprotective function.[12,19,26] It has been postulated that resident macrophages are more likely to have a role in tissue repair processes in cardiac injury.[12] However, in the present study, immunohistochemistry showed that macrophages in the focal lesions expressed TGF-β, ICAM-1, VEGF, and, less abundantly, its receptor Flk1. These findings suggest a dual function (ie. both a reparative and an inflammatory role) in canine DCM. In rats, ICAM-1, a cell adhesion molecule critical for leukocyte recruitment, mediates adhesion of macrophages to cardiomyocytes.[6,44] Such macrophage adherence can result in decreased cardiomyocyte contractility via the expression of TNF-α, oxygen free radicals, and nitric oxide.[44] Laser microdissection with subsequent qPCR undertaken on the myocardium of 1 dog and immunohistochemistry provide strong evidence that cardiomyocytes produce ICAM-1, cytokines, and

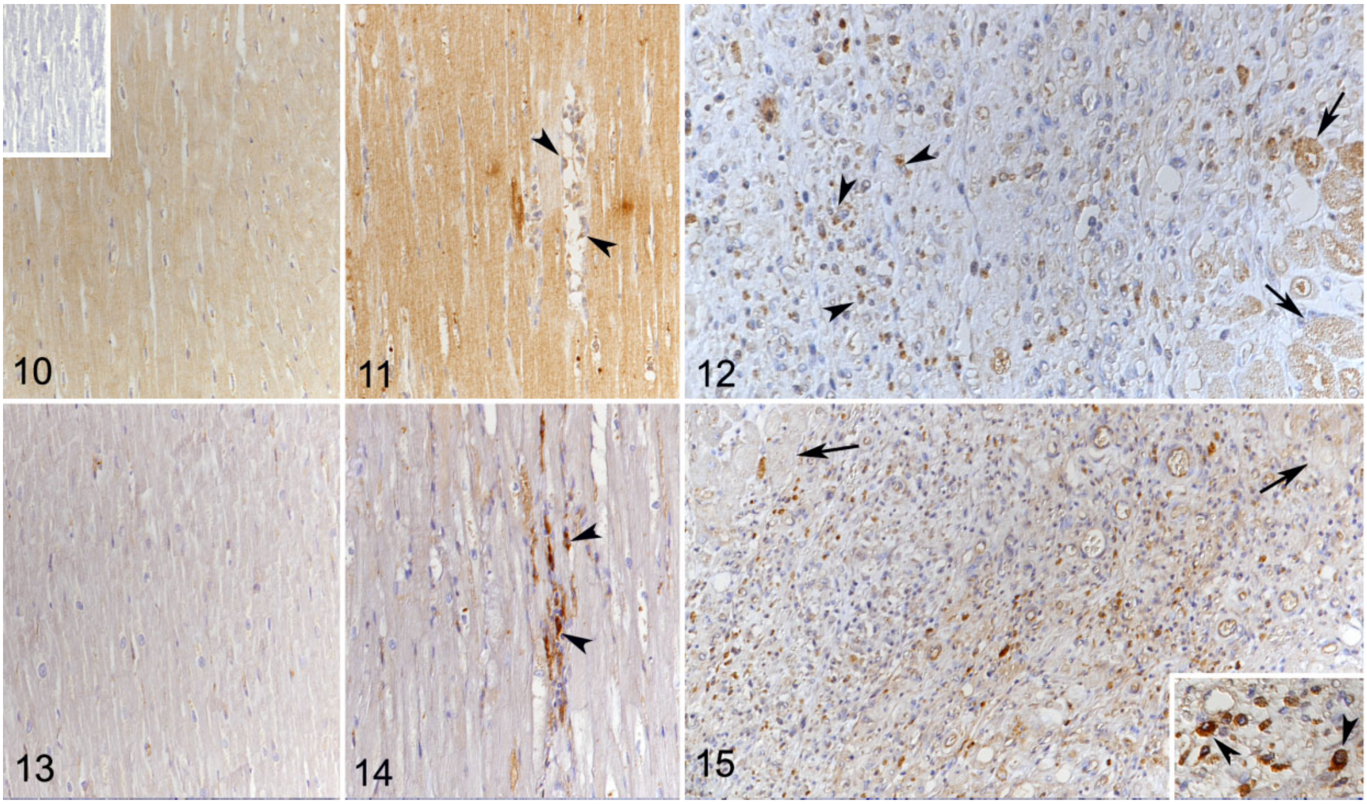

Figures 10–12. Expression of intracellular adhesion molecule 1 (ICAM-1) in the myocardium. Immunohistochemistry, hematoxylin counterstain. **Figure 10**. Control heart, dog No. 2.2. Cardiomyocytes show weak ICAM-1 expression. Inset: No reaction is seen in a negative control slide. **Figures 11 and 12.** Dilated cardiomyopathy (DCM), heart, dog No. 1.15. **Figure 11.** Cardiomyocytes show moderate ICAM-1 expression. The interstitial cells exhibit only very weak staining (arrowheads). **Figure 12.** A substantial proportion of the mononuclear cells in the focal lesion exhibit ICAM-1 expression (arrowheads). Arrows: cardiomyocytes. **Figures 13–15.** Expression of transforming growth factor β (TGF-β) in the myocardium. Immunohistochemistry, hematoxylin counterstain. **Figure 13.** Control heart, dog No. 2.1. Cardiomyocytes show no or very weak TGF-β expression. **Figures 14–15.** DCM, heart, dog No. 1.15. **Figure 14.** Cardiomyocytes exhibit very weak to weak TGF-β expression, whereas the interstitial cells are often strongly TGF-β-positive (arrowheads). **Figure 15.** A substantial proportion of the mononuclear cells in the focal lesion exhibit ICAM expression (inset: arrowheads). Arrows: cardiomyocytes.

remodeling enzymes, such as IL-8, TNF-α, TGF-β, MMP-2, TIMP-1, and TIMP-2. This suggests that both macrophages and cardiomyocytes might contribute to cardiomyocyte damage and/or dysfunction and the pathogenic process in dogs with DCM. ICAM-1 and cytokine upregulation also suggest an inflammatory state of the DCM myocardium. Inflammatory cytokines, such as TNF-α and IL-1, and chemokines regulate collagen turnover. These cytokines are involved in the dysregulation of MMP and TIMP expression[8,10] and inhibition of collagen degradation. This contributes to fibrosis, as observed in the dogs with DCM, and to decreased myocardial contractility and progression of heart failure, as reported for human DCM.[31,46,47] In particular, upregulation of MMP-2, TIMP-1, and TIMP-2 has been described in nonischemic human DCM and in experimental conditions in dogs,[35,36,45,51] which is similar to the increase of MMP-2 and TIMP-1 found in the DCM dogs. Furthermore, TGF-β that was expressed by cardiomyocytes as well as by lesional and interstitial macrophages might contribute to the increase in collagen observed in the DCM dogs. Cardiomyocytes under stress conditions or undergoing necrosis are known to be able to contribute to fibrosis through the production of TGF-β.[21] TGF-β exerts profibrotic effects through the proliferation and differentiation of fibroblasts into myofibroblasts,[5,9,10] cells that were likely present both among the interstitial macrophage population and within the focal cell-rich lesions in the canine DCM myocardium.

In addition to the macrophage infiltration, the focal cell-rich lesions exhibited abundant small vessels indicative of neovascularization, whereas collagen deposition was limited. Individual degenerating/necrotic cardiomyocytes were found in the periphery of or entrapped within the lesions. The morphological evidence of neovascularization was associated with VEGF expression within infiltrating cells (most likely macrophages) in the lesions. These macrophages also produce TGF-β,[25,54] which, next to hypoxia, further stimulates VEGF production.[25,50]

Interestingly, the macrophages with higher proangiogenic potential have been shown to belong to the anti-inflammatory subset of macrophages and might therefore be involved in a repair attempt of the observed lesions.[30]

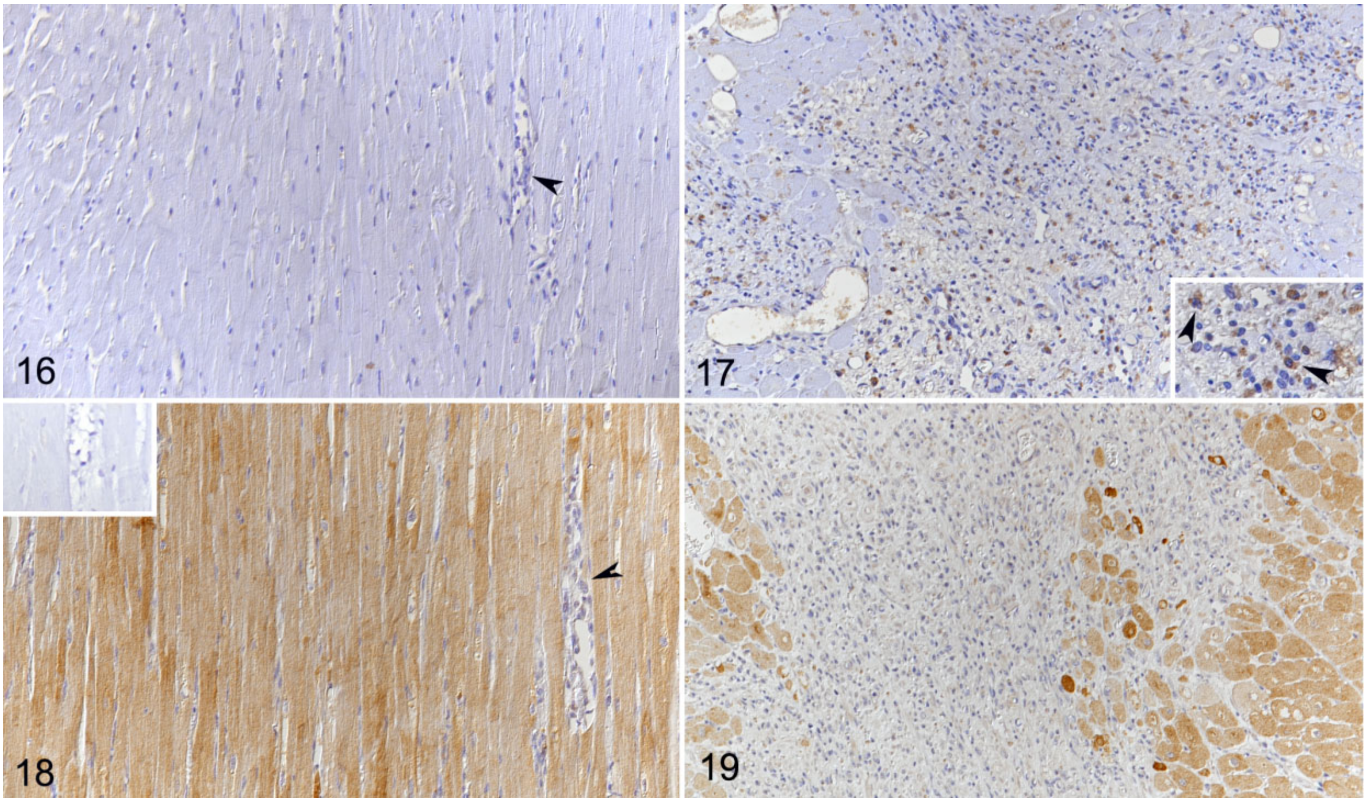

Figures 16–17. Dilated cardiomyopathy (DCM), heart, dog No. 1.15. Expression of vascular endothelial growth factor (VEGF) in the myocardium. Immunohistochemistry, hematoxylin counterstain. **Figure 16.** Cardiomyocytes as well as the interstitial cells (arrowheads) are VEGF negative. **Figure 17.** A substantial proportion of the mononuclear cells in the focal lesion exhibit VEGF expression (inset: arrowheads). **Figures 18–19.** DCM, heart, dog No. 1.15. Expression of the VEGF receptor Flk1 in the myocardium. Immunohistochemistry, hematoxylin counterstain. **Figure 18.** Cardiomyocytes exhibit moderate Flk1 expression, whereas the interstitial cells are Flk1 negative (arrowhead). Inset: No reaction is seen in a negative control slide. **Figure 19.** The cells in the focal lesion are also Flk1 negative.

We found evidence of substantial expression of the VEGF receptor Flk-1 by cardiomyocytes in DCM, with particular intensity in cardiomyocytes entrapped in the lesions. When binding to Flk-1, VEGF exerts its angiogenetic properties; this interaction might have further contributed to the observed new vessel formation.[50] Morphologically, the focal lesions resemble chronic myocardial infarcts:[14] infarct healing is associated, particularly in the dog, with an intense angiogenic response.[7] Considering that we did not observe changes that would directly explain these lesions, and taking into account the described diffuse changes, it appears most likely that the focal lesions are a consequence of focal cardiomyocyte necrosis as a result of reduced tissue perfusion. The latter might be the result of the increased distance between blood vessels and cardiomyocytes due to interstitial edema (indicated by the overall widening of the interstitial space) and collagen deposition, or it might also derive from the reduced oxygen tension characteristic of the microenvironment of a chronically inflamed tissue.[49]

In summary, canine DCM is associated with diffuse myocardial remodeling processes and focal lesions in the majority of dogs. Both macrophages and cardiomyocytes might actively contribute to the pathogenic process through the production of cytokines, adhesion molecules, and remodeling enzymes, which eventually leads to cardiac dilation and impaired cardiac function.

Interestingly, we found similar changes (ie, generalized diffuse remodeling and focal lesions) with cardiomyocyte degeneration, increased fibrosis, macrophages, and neovascularization in cats with hypertrophic cardiomyopathy, a disease with a very different phenotype.[33] The resemblance of these results suggests similar pathophysiological processes. Further investigations are required to explain how these processes result in diseases with different structural and functional presentations and which are the roles of macrophages and cardiomyocytes, since both appear primarily involved in the pathogenesis of both canine DCM and feline hypertrophic cardiomyopathy.

Acknowledgements

We are grateful to the technical staff in the Histology Laboratory, Institute of Veterinary Pathology, Vetsuisse Faculty, University of Zurich, for excellent technical support and to Prof. Mark Oyama, School of Veterinary Medicine, University of Pennsylvania, for providing us with the mouse anti-canine ICAM antibody. Thanks are due to Dr Giovanni Pellegrini, Laboratory for Animal Model Pathology, Institute of Veterinary Pathology, Vetsuisse Faculty, University of Zurich, for his support toward the morphometric study.

Declaration of Conflicting Interests

The author(s) declared no potential conflicts of interest with respect to the research, authorship, and/or publication of this article.

Funding

The author(s) disclosed receipt of the following financial support for the research, authorship, and/or publication of this article: The RT-qPCR work was supported by a grant from the University of Liverpool and a NSERC discovery grant (RGPIN-2017-04399) from the government of Canada.

ORCID iD

Sarah Kitz https://orcid.org/0000-0002-9335-9615
Anja Kipar https://orcid.org/0000-0001-7289-3459

References

1. Anker SD, Von Haehling S. Inflammatory mediators in chronic heart failure: an overview. *Heart*. 2004;**90**(4):464–470.
2. Beltrami CA, Finato N, Rocco M, et al. The cellular basis of dilated cardiomyopathy in humans. *J Mol Cell Cardiol*. 1995;**27**(1):291–305.
3. Cohn JN, Ferrari R, Sharpe N. Cardiac remodeling-concepts and clinical implications: a consensus paper from an International Forum on Cardiac Remodeling. *J Am Coll Cardiol*. 2000;**35**(3):569–582.
4. Dambach DM, Lannon A, Sleeper MM, et al. Familial dilated cardiomyopathy of young Portuguese water dogs. *J Vet Intern Med*. 1999;**13**(1):65–71.
5. Darby IA, Laverdet B, Bonté F, et al. Of mice and dogs: species-specific differences in the inflammatory response following myocardial infarction. *Clin Cosmet Investig Dermatol*. 2014;**7**:301–311.
6. Davani EY, Dorscheid DR, Lee CH, et al. Novel regulatory mechanism of cardiomyocyte contractility involving ICAM-1 and the cytoskeleton. *Am J Physiol Heart Circ Physiol*. 2004;**287**(3):H1013–H1022.
7. Dewald O, Ren G, Duerr GD, et al. Of mice and dogs: species-specific differences in the inflammatory response following myocardial infarction. *Am J Pathol*. 2004;**164**(2):665–677.
8. Dixon JA, Spinale FG. Myocardial remodeling: cellular and extracellular events and targets. *Annu Rev Physiol*. 2011;**73**:47–68.
9. Dobaczewski M, Chen W, Frangogiannis NG. Transforming growth factor (TGF)-β signaling in cardiac remodeling. *J Mol Cell Cardiol*. 2011;**51**(4):600–606.
10. Dobaczewski M, Gonzalez-Quesada C, Frangogiannis NG. The extracellular matrix as a modulator of the inflammatory and reparative response following myocardial infarction. *J Mol Cell Cardiol*. 2010;**48**(3):504–511.
11. Dukes-McEwan J, Borgarelli M, Tidholm A, et al. Proposed guidelines for the diagnosis of canine idiopathic dilated cardiomyopathy. *J Vet Cardiol*. 2003;**5**(2):7–19.
12. Epelman S, Lavine KJ, Beaudin AE, et al. Embryonic and adult-derived resident cardiac macrophages are maintained through distinct mechanisms at steady state and during inflammation. *Immunity*. 2014;**40**(1):91–104.
13. Everett RM, McGann J, Wimberly HC, et al. Dilated cardiomyopathy of Doberman Pinschers: retrospective histomorphologic evaluation of heart from 32 cases. *Vet Pathol*. 1999;**36**(3):221–227.
14. Falk T, Jönsson L. Ischaemic heart disease in the dog: a review of 65 cases. *J Small Anim Pract*. 2000;**41**(3):97–103.
15. Fonfara S, Hetzel U, Tew SR, et al. Expression of matrix metalloproteinases, their inhibitors, and lysyl oxidase in myocardial samples from dogs with end-stage systemic and cardiac diseases. *Am J Vet Res*. 2013;**74**(2):216–223.
16. Fonfara S, Hetzel U, Tew SR, et al. Myocardial cytokine expression in dogs with systemic and naturally occurring cardiac diseases. *Am J Vet Res*. 2013;**74**(3):408–416.
17. Fonfara S, Tew SR, Cripps P, et al. Increased blood mRNA expression of inflammatory and anti-fibrotic markers in dogs with congestive heart failure. *Res Vet Sci*. 2012;**93**(2):879–885.
18. Frangogiannis NG. Regulation of the inflammatory response in cardiac repair. *Circ Res*. 2012;**110**(1):159–173.
19. Frangogiannis NG. Inflammation in cardiac injury, repair and regeneration. *Curr Opin Cardiol*. 2015;**30**(3):240–245.
20. Frangogiannis NG. Emerging roles for macrophages in cardiac injury: cytoprotection, repair, and regeneration. *J Clin Invest*. 2015;**125**(8):2927–2930.
21. Frangogiannis NG. Fibroblasts and the extracellular matrix in right ventricular disease. *Cardiovasc Res*. 2017;**113**(12):1453–1464.
22. Frantz S, Nahrendorf M. Cardiac macrophages and their role in ischemic heart disease. *Cardiovasc Res*. 2014;**102**(2):1–9.
23. Fujiu K, Wang J, Nagai R. Cardioprotective function of cardiac macrophages. *Cardiovasc Res*. 2014;**102**(2):232–239.
24. Hanna N, Cardin S, Leung TK, et al. Differences in atrial versus ventricular remodeling in dogs with ventricular tachypacing-induced congestive heart failure. *Cardiovasc Res*. 2004;**63**(2):236–244.
25. Harmey JH, Dimitriadis E, Kay E, et al. Regulation of macrophage production of vascular endothelial growth factor (VEGF) by hypoxia and transforming growth factor beta-1. *Ann Surg Oncol*. 1998;**5**(3):271–278.
26. Hulsmans M, Sam F, Nahrendorf M. Monocyte and macrophage contributions to cardiac remodeling. *J Mol Cell Cardiol*. 2016;**93**:149–155.
27. Janus I, Kandefer-Gola M, Ciaputa R, et al. The immunohistochemical evaluation of selected markers in the left atrium of dogs with end-stage dilated cardiomyopathy and myxomatous mitral valve disease—a preliminary study. *Ir Vet J*. 2016;**69**:18.
28. Janus I, Noszczyk-Nowak A, Nowak M, et al. A comparison of the histopathologic pattern of the left atrium in canine dilated cardiomyopathy and chronic mitral valve disease. *BMC Vet Res*. 2016;**12**:3.
29. Janus I, Nowak M, Madej JA. Pathomorphological changes of the myocardium in canine dilated cardiomyopathy (DCM). *Bull Vet Inst Pulawy*. 2015;**59**(1):135–142.
30. Jetten N, Verbruggen S, Gijbels MJ, et al. Anti-inflammatory M2, but not pro-inflammatory M1 macrophages promote angiogenesis in vivo. *Angiogenesis*. 2014;**17**(1):109–118.
31. Kim HE, Dalal SS, Young E, et al. Disruption of the myocardial extracellular matrix leads to cardiac dysfunction. *J Clin Invest*. 2000;**106**(7):857–866.
32. Kipar A, Baumgärtner W, Kremmer E, et al. Expression of major histocompatibility complex class II antigen in neoplastic cells of canine cutaneous histiocytoma. *Vet Immunol Immunopathol*. 1998;**62**(1):1–13.
33. Kitz S, Fonfara S, Hahn S, et al. Feline hypertrophic cardiomyopathy, the consequence of cardiomyocyte-initiated and macrophage-driven remodeling processes? *Vet Pathol*. 2019;**56**(4):565–575.
34. Lee YR, Kang MH, Park HM. Anthracycline-induced cardiomyopathy in a dog treated with epirubicin. *Can Vet J*. 2015;**56**(6):571–574.
35. Li YY, McTiernan CF, Feldman AM. Interplay of matrix metalloproteinases, tissue inhibitors of metalloproteinases and their regulators in cardiac matrix remodeling. *Cardiovasc Res*. 2000;**46**(2):214–224.
36. Lin JM, Lai LP, Lin CS, et al. Left Ventricular extracellular matrix remodeling in dogs with right ventricular apical pacing. *J Cardiovasc Electrophysiol*. 2010;**21**(10):1142–1149.
37. Lobo L, Carvalheira J, Canada N, et al. Histologic characterization of dilated cardiomyopathy in Estrela Mountain Dogs. *Vet Pathol*. 2010;**47**(4):637–642.
38. Martin MWS, Stafford Johnson MJ, Celona B. Canine dilated cardiomyopathy: a retrospective study of signalment, presentation and clinical findings in 369 cases. *J Small Anim Pract*. 2009;**50**(1):23–29.
39. Meurs KM, Fox PR, Norgard M, et al. A prospective genetic evaluation of familial dilated cardiomyopathy in the Doberman Pinscher. *J Vet Intern Med*. 2007;**21**(5):1016–1020.
40. Meurs KM, Stern JA, Sisson DD, et al. Association of dilated cardiomyopathy with the striatin mutation genotype in boxer dogs. *J Vet Intern Med*. 2013;**27**(6):1437–1440.
41. Oyama MA, Chittur SV. Genomic expression patterns of mitral valve tissues from dogs with degenerative mitral valve disease. *Am J Vet Res*. 2006;**67**(8):1307–1318.

42. Philipp U, Vollmar A, Häggström J, et al. Multiple loci are associated with dilated cardiomyopathy in Irish Wolfhounds. *PLoS One*. 2012;**7**(6):1–6.
43. Sandusky GE, Capen CC, Kerr KM. Histological and ultrastructural evaluation of cardiac lesions in idiopathic cardiomyopathy in dogs. *Can J Comp Med*. 1984;**48**(1):81–86.
44. Simms MG, Walley KR. Activated macrophages decrease rat cardiac myocyte contractility: importance of ICAM-1-dependent adhesion. *Am J Physiol*. 1999;**277**(1):H253–H260.
45. Simpson S, Edwards J, Ferguson-Mignan TF, et al. Genetics of human and canine dilated cardiomyopathy. *Int J Genomics*. 2015;**2015**:204823.
46. Spinale FG.Matrix metalloproteinases: Regulation and dysregulation in the failing heart. *Circ Res*. 2002;**90**(5):520–530.
47. Spinale FG. Myocardial matrix remodeling and the matrix metalloproteinases: influence on cardiac form and function. *Physiol Rev*. 2007;**87**(4):1285–1342.
48. Stephenson HM, Fonfara S, López-Alvarez J, et al. Screening for dilated cardiomyopathy in Great Danes in the United Kingdom. *J Vet Intern Med*. 2012;**26**(5):1140–1147.
49. Szade A, Grochot-Przeczek A, Florczyk U, et al. Cellular and molecular mechanisms of inflammation-induced angiogenesis. *IUBMB Life*. 2015;**67**(3):145–159.
50. Taimeh Z, Loughran J, Birks EJ, et al. Vascular endothelial growth factor in heart failure. *Nat Rev Cardiol*. 2013;**10**(9):519–530.
51. Thomas CV, Coker ML, Zellner JL, et al. Increased matrix metalloproteinase activity and selective upregulation in LV myocardium from patients with end-stage dilated cardiomyopathy. *Circulation*. 1998;**97**(17):1708–1715.
52. Tidholm A, Häggström J, Borgarelli M, et al. Canine idiopathic dilated cardiomyopathy. Part I: aetiology, clinical characteristics, epidemiology and pathology. *Vet J*. 2001;**162**(2):92–107.
53. Tidholm A, Jönsson L. Histologic characterization of canine dilated cardiomyopathy. *Vet Pathol*. 2005;**42**(1):1–8.
54. Uchida N, Nagai K, Sakurada Y, et al. Distribution of VEGF and flt-1 in the normal dog tissues. *J Vet Med Sci*. 2008;**70**(11):1273–1276.
55. Vollmar AC, Aupperle H. Cardiac pathology in Irish wolfhounds with heart disease. *J Vet Cardiol*. 2016;**18**(1):57–70.
56. Wess G, Schulze A, Butz V, et al. Prevalence of dilated cardiomyopathy in Doberman Pinschers in various age groups. *J Vet Intern Med*. 2010;**24**(3):1–6.